

Lump waves from the degeneration of lump chains in the (2+1)-dimensional Boussinesq-type equation

Lili Hou(侯丽丽), Biao Li(李彪)

Citation: Chin. Phys. B. 35, 090202 (2026). DOI: 10.1088/1674-1056/ae6d99 | CSTR: 32038.14.CPB.ae6d99
http://cpb.iphy.ac.cn; http://iopscience.iop.org/cpb

What follows is a list of articles you may be interested in

Abundant invariant solutions of extended (3+1)-dimensional KP–Boussinesq equation

Hengchun Hu(胡恒春), Jiali Kang(康佳丽)
Chin. Phys. B. 33, 110206 (2024). DOI: 10.1088/1674-1056/ad7fd1

Soliton propagation for a coupled Schrödinger equation describing Rossby waves

Li-Yang Xu(徐丽阳), Xiao-Jun Yin(尹晓军), Na Cao(曹娜), Shu-Ting Bai(白淑婷)
Chin. Phys. B. 32, 070202 (2023). DOI: 10.1088/1674-1056/acb9e5

A nonlocal Boussinesq equation: Multiple-soliton solutions and symmetry analysis

Xi-zhong Liu(俞军), Jun Yu(俞军)
Chin. Phys. B. 31, 050201 (2022). DOI: 10.1088/1674-1056/ac43a7

A meshless algorithm with the improved moving least square approximation for nonlinear improved Boussinesq equation

Yu Tan(谭渝), Xiao-Lin Li(李小林)
Chin. Phys. B. 30, 010201 (2021). DOI: 10.1088/1674-1056/abaed7

Truncated series solutions to the (2+1)-dimensional perturbed Boussinesq equation by using the approximate symmetry method

Xiao-Yu Jiao(焦小玉)
Chin. Phys. B. 27, 100202 (2018). DOI: 10.1088/1674-1056/27/10/100202

SPECIAL TOPIC — Nonlinear localized waves: Theory, methods and applications

Lump waves from the degeneration of lump chains in the $(2+1)$-dimensional Boussinesq-type equation

Lili Hou(侯丽丽) and Biao Li(李彪)[†]

School of Mathematics and Statistics, Ningbo University, Ningbo 315211, *China*

(Received 19 March 2026; revised manuscript received 27 April 2026; accepted manuscript online 14 May 2026)

We construct lump waves of the Boussinesq-type equation through two distinct approaches and present the corresponding figures. In the first method, lump chains are reduced to lump waves in two steps. Initially, appropriate parameters are selected to control the periods and amplitudes of the lump chains. When the periods and amplitudes of all lump chains tend to be identical, the lump chains exhibit coupling and form coupled lump chains. Then, as the periods of the coupled lump chains approach infinity, these coupled lump chains are finally reduced to lump waves. In the second approach, using the improved long-wave limit method, we directly reduce lump chains to lump waves.

Keywords: lump chains, Boussinesq-type equation, lump waves

PACS: 02.30.Ik, 02.30.Jr, 05.45.Yv

DOI: 10.1088/1674-1056/ae6d99 **CSTR:** 32038.14.CPB.ae6d99

1. Introduction

The study of nonlinear partial differential equations (NPDEs) can be traced back to the 19th century. As an important branch of modern mathematics, NPDEs[1–4] not only have profound theoretical connotations but also have extensive applications in various fields of science and engineering. Boussinesq-type equations, as an important class of partial differential equations, play a significant role not only in theoretical studies in mathematics but also in practical applications. Their nonlinear and dispersive characteristics enable them to accurately describe the complex behavior of shallow water waves, and they are widely used in fields such as coastal engineering and water wave simulation. In 1872, Boussinesq[5] established the perturbation expansion theory while studying the free-boundary problem of incompressible and irrotational water waves. He derived several nonlinear evolution equations and systems of equations to simulate the propagation of small-amplitude long waves on the water surface. He also provided a scientific explanation for the existence of waves and pointed out the use of Lyapunov's method to describe wave stability. He noted that these equations have soliton solutions, which laid a solid foundation for subsequent research on Boussinesq equations. The classical Boussinesq equations were originally proposed by Zakharov[6]

$$u_{tt}-u_{xx}+\alpha u_{xxxx}=\beta(u^2)_{xx}, \tag{1}$$

where $u=u(x,t)$ represents the fluid velocity, the subscripts x and t denote partial derivatives with respect to x and t, respectively, and the constants α and β depend on the depth of the fluid and the characteristic speed of long waves. When $\alpha\geq 0$, Eq. (1) is referred to as the "good" Boussinesq equation. By applying the Fourier transform, we can demonstrate that it is linearly stable. When $\alpha<0$, Eq. (1) is known as the "bad" Boussinesq equation. Bona and Sachs[7] studied a class of classical Boussinesq equations

$$u_{tt}=u_{xx}-(u^2+u_{xx})_{xx}, \tag{2}$$

and proved that the corresponding initial-boundary-value problem is always locally well-posed; they also showed that its special solitary-wave solutions are nonlinearly stable for a range of propagation speeds. Deift[8] applied the inverse scattering method to the following problem:

$$u_{tt}=3u_{xxxx}+u_{xx}-12(u^2)_{xx}. \tag{3}$$

Boussinesq-type equations possess a wide variety of solutions. Among them, lump solutions have become increasingly popular. In 1976, the first lump solution made its appearance. Petviashvili[9] proposed an integral iterative method to solve for the two-dimensional steady-state solution $u(x-ct,y)$, converging to an elliptical, algebraically decaying localized wave, where the product of amplitude and width is a constant, which is distinctly different from the exponentially decaying KdV soliton. The solution was named "lump", emphasizing its two-dimensional finite-mass characteristic. In 1980, Satsuma and Ablowitz[10] discovered, through the Hirota bilinear method, that in the long-wave limit, the τ-function degenerates into a polynomial, providing a nonsingular analytic solution. In 1986, Matveev and Salle[11] to publish a series of preprints, providing explicit formulas for deriving N-lumps from N-solitons of the Kadomtsev–Petviashvili (KP) equation. They

[†]Corresponding author. E-mail: libiao@nbu.edu.cn

© 2026 Chinese Physical Society and IOP Publishing Ltd. All rights, including for text and data mining, AI training, and similar technologies, are reserved.

demonstrated that the τ-function degenerates into a polynomial determinant in the long-wave limit, achieving the first analytical construction of multi-lump bound states. Subsequently, he published the classic monograph "Darboux Transformations and Solitons", which systematically summarized the unified framework of Darboux transformations for generating lumps, line-solitons, and breathers. This work is regarded by later generations as the standard reference for lump theory. Zhang *et al.*[12–15] made significant contributions to the study of lump solutions and published several papers on the topic. Li *et al.*[16,17] determined interacting lumps for the $(2+1)$-dimensional generalized Korteweg–de Vries equation via degeneracy of lump chains and validated degenerate lump solutions for the $(2+1)$-dimensional Yu–Toda–Sasa–Fukuyama equation. Zhou[18] introduced the $(2+1)$-dimensional Boussinesq-type equation and obtained its lump solution. Bound states composed of multiple lumps are referred to as "lump molecules", which consist of $\frac{n(n+1)}{2}$ lumps. A periodic lump chain can degenerate into a single lump when the period tends to infinity. Here, we will improve upon the long-wave-limit method to demonstrate how lump patterns can be more easily derived from N-soliton solutions by appropriately selecting parameters. This method is also applicable to other integrable equations.

The remaining sections of this paper are organized as follows: In Section 2, we first introduce new variables to reduce the $(2+1)$-dimensional Boussinesq-type equation to a $(1+1)$-dimensional equation. The reduced equation is also a Boussinesq-type equation. We then solve for the N-soliton solution of the $(1+1)$-dimensional Boussinesq-type equation using the Hirota bilinear method. In Section 3, we first review how to obtain a lump chain solution from the double soliton solution of the $(1+1)$-dimensional Boussinesq-type equation. Then, we demonstrate the process of a lump chain degenerating into a lump wave using two methods. The first method is to first degenerate the lump chain into a coupled lump chain and then further degenerate it into a lump wave by selecting appropriate parameters. The second method involves the use of the improved long-wave-limit approach. By appropriately selecting parameters, a lump wave can be directly and efficiently obtained from the lump chain. In Sections 4 and 5, we apply the same approaches to show how higher-order lump waves can be obtained. In the conclusion, we provide a summary of the results.

2. The N-soliton solution to Boussinesq-type equation

The original equation is a generalized $(2+1)$-dimensional Boussinesq equation[19]

$$u_{xxxx}+4u_x^2+4uu_x-u_{xx}-u_{tt}-\tfrac{1}{2}u_{yy}=0. \tag{4}$$

Introducing the characteristic coordinates

$$\xi=x,\quad \eta=y+\sqrt{\tfrac{1}{2}}t, \tag{5}$$

reduces the three-dimensional equation to a two-dimensional Boussinesq-type equation by means of the chain rule

$$u_{\xi\xi\xi\xi}+2(u^2)_{\xi\xi}-u_{\xi\xi}-u_{\eta\eta}=0, \tag{6}$$

using the bilinear derivative method

$$u=3\frac{\partial^2}{\partial^2\xi}\ln f(\xi,\eta). \tag{7}$$

Equation (7) can be cast into the following bilinear form:

$$(D_\xi^4-D_\xi^2-D_\eta^2)f\cdot f=0. \tag{8}$$

The operators are defined as follows:[20]

$$\begin{aligned}D_\xi^nD_\eta^m(f\cdot g)\;=\;&\left(\frac{\partial}{\partial\xi}-\frac{\partial}{\partial\xi'}\right)^n\left(\frac{\partial}{\partial\eta}-\frac{\partial}{\partial\eta'}\right)^m\\&\times f(\xi,\eta)g(\xi',\eta')|\xi=\xi',\;\;\eta=\eta'.\end{aligned} \tag{9}$$

The N-soliton solution of Eq. (6) can be expressed in terms of the solution of Eq. (8)

$$f=\sum\exp\left(\sum_{i=1}^{N}v_iX_i+\sum_{i<j}^{N}v_iv_jA_{ij}\right), \tag{10}$$

where

$$\begin{aligned}&X_j=k_j\xi+w_j\eta+X_j^{(0)},\;w_j=\theta_jk_j\sqrt{k_j^2-1},\\&\mathrm{e}^{A_{ij}}=-\frac{(k_1-k_2)^4-(k_1-k_2)^2-(w_1-w_2)^2}{(k_1+k_2)^4-(k_1+k_2)^2-(w_1+w_2)^2},\end{aligned} \tag{11}$$

where $\theta_j=\pm1, j=1,2,\ldots,M$, and the leading symbol $\sum$ in Eq. (10) indicates summation over the entire set of binary indices $v_1,v_2,\ldots,v_N\in\{0,1\}$.

Exploiting the bilinear structure of Eq. (10), we proceed to derive the lump waves of interest.

3. Degeneration of a lump chain into a single lump wave

In what follows, we shall concentrate on the mechanism by which a lump chain is reduced to a lump wave. This phenomenon has been extensively investigated by numerous scholars.[21–25] Lump chains are another type of soliton. They consist of a series of lump waves with identical velocities, which are uniformly distributed along a straight line. Owing to their inherent spatial periodicity, these solutions are widely known as periodic solitons in the relevant studies. When $X_1=X_2^*$, we can obtain a lump chain from the degenerate two-soliton solution in Ref. [21], and the solution is nonsingular if $|k_j|\le 1/2$. Specifically, upon restricting the parameters in Eq. (10) to the sector $0<k_1=k_2<1/2$, $\theta_1=1$, $\theta_2=-1$, we can derive the first-order lump-chain solution

$$u=3\frac{\partial^2}{\partial\xi^2}\ln\left[\cosh\left(X_{1,R}+\frac{\ln A_{12}}{2}\right)+\frac{\cos X_{1,I}}{\sqrt{A_{12}}}\right], \tag{12}$$

where $X_1 = k_1\xi + i\omega_1\eta + X_1^{(0)}$, $\omega_1 = k_1\sqrt{1-k_1^2}$, $A_{12} = \ln\left(\frac{4\omega_1^2}{16k_1^4-4k_1^2}\right)$, and $X_{1,R}$ and $X_{1,I}$ represent, respectively, the real and imaginary components of the complex quantity X.

From Eq. (12), the position of the lump chain on the (ξ,η)-plane and its extreme values are given by the following expressions, respectively

$$X_{1,R} + \frac{\ln A_{12}}{2} = 0, \quad u_{max} = \frac{3k_1^2}{1+\mathrm{e}^{-\frac{A_{12}}{2}}}\cos X_{1,I},$$

consequently, the spatial period and the maximum amplitude of the lump chain are obtained as follows when $\cos X_{1,I} = -1$

$$T = \frac{2\pi}{k_1\sqrt{1-k_1^2}}, \quad A = \frac{3k_1^2}{1-\mathrm{e}^{-\frac{A_{12}}{2}}}.$$

With different parameters chosen, the figures of the first-order lump chain are presented in Fig. 1. We perform a Taylor expansion of Eq. (12) around $k_1 \to 0$

$$\begin{aligned}&\cosh\left(X_{1,R} + \frac{\ln A_{12}}{2}\right) + \frac{\cos X_{1,I}}{\sqrt{A_{12}}}\\ \xrightarrow{k_1\to 0}\ &\left[\frac{1}{2}\xi^2 - \frac{3}{2} - \cos\left(X_{1,I}^{(0)} - \frac{1}{2}\cos\left(X_{1,I}^{(0)}\right)\eta^2\right)\right]k_1^2\\ &-\frac{1}{2}\sin(X_{1,I}^{(0)})\eta k_1 + \cos(X_{1,I}^{0}) + 1 + O(k_1^3). \qquad (13)\end{aligned}$$

Let $X_{1,I}^{(0)} = \pi$ and neglect $O(k_1^3)$; we can obtain the first-order lump solution

$$u = 3\frac{\partial^2}{\partial\xi^2}\ln(\xi^2+\eta^2+3) = \frac{6\eta^2-6\xi^2+18}{(\eta^2+\xi^2+3)^2}. \qquad (14)$$

The figure of the first-order lump wave are shown in Fig. 2. The exact analytical solution[23,26] corresponding to Eq. (13) can also be obtained by the long-wave limit method. The advantage of this method is that it avoids the aforementioned complicated analysis and thus allows one to obtain rational solutions quickly. The parameters appearing in Eq. (10) are assigned the values

$$N = 2, \quad \theta_1 = 1, \quad \theta_2 = -1, \quad k_1 = M_1\theta,$$

$$k_2 = M_2\theta, \quad X_1^{(0)} = X_2^{(0)} = \mathrm{i}\pi, \qquad (15)$$

then Eq. (10) can be expanded into the following series when $\theta \to 0$:

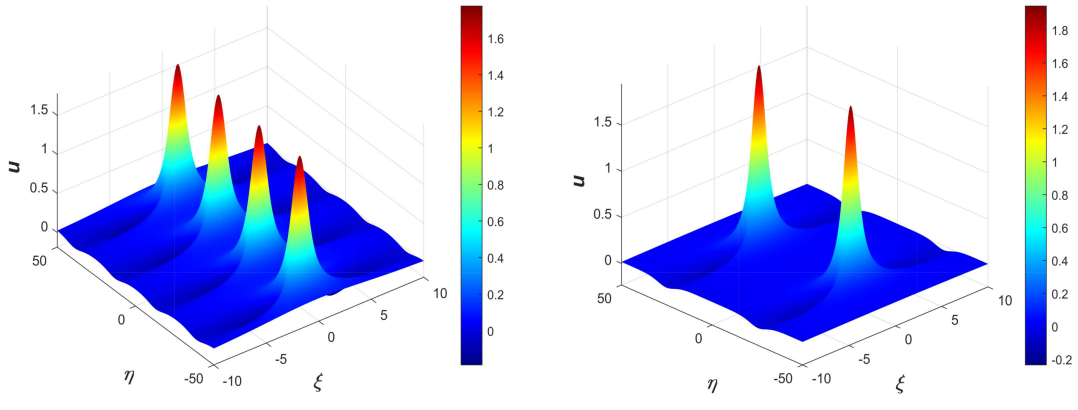
$$f = f^{(0)} + f^{(1)}\theta + f^{(2)}\theta^2 + O(\theta^3). \qquad (16)$$

By setting the coefficients of the initial two terms to zero, we can obtain $\mathrm{e}^{X_1^{(0)}} = \mathrm{e}^{X_2^{(0)}} = -1$. Therefore, the auxiliary function Eq. (10) can be reduced to a new auxiliary function

$$f = M_1M_2(\xi^2+\eta^2+3)\theta^2. \qquad (17)$$

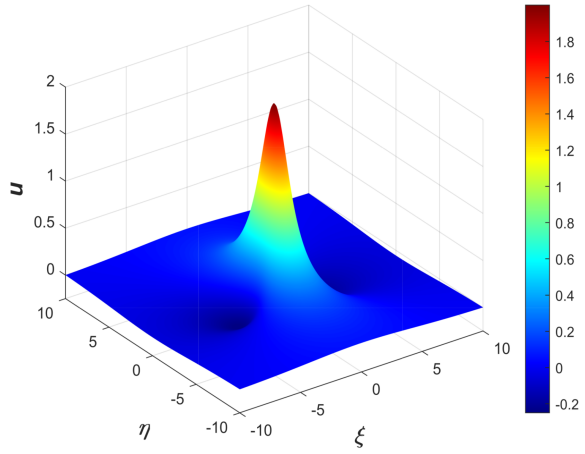
Under the Hirota transformation, the factors $M_1M_2\theta^2$ appearing in Eq. (17) exert no influence on the solution of the equation. Equivalently, Eqs. (14) and (16) possess exactly the same solutions. Therefore, we can conclude that deriving Eq. (14) from Eq. (10) is equivalent to the period of the lump chain tending to infinity. In the next sections, we will show how to identify the key restrictive conditions in Eq. (15) and use them to derive lump-wave molecules directly from lump-chain molecules.

This chapter is inspired by the seminal work of Wang *et al.*[27] Our work is analogous to reducing the breather solution of the nonlinear Schrödinger equation to higher-order rogue waves. This concept can also be extended to nonlinear Boussinesq-type systems for constructing lump-wave molecules. By imposing appropriate constraints and perturbations on the N-soliton solution displayed in Eq. (10), one can reduce the lump chains to an intermediate state and then further obtain the lumps. However, when Yuan *et al.* attempted to implement this idea,[22] they failed because the authors in question reduced M-lump chains to only M-lumps, instead of the required $M(M+1)/2$ lumps. In fact, they simply let the period of each individual lump chain tend to infinity separately, thereby obtaining only the ordinary scattering of lumps.



(a) (b)

Fig. 1. (a) The first-order lump chain governed by Eq. (12) is characterized by the parameters $k_1 = 1/4$ and $X_1^{(0)} = -\frac{1}{2}\ln(\frac{8}{7})$; (b) the first-order lump chain governed by Eq. (12) is characterized by the parameters $k_2 = 1/8$ and $X_2^{(0)} = -\frac{1}{2}\ln(\frac{21}{20})$.



(a)

Fig. 2. The first-order lump wave described by Eq. (14).

Lump waves can be derived from lump chains via two distinct routes: first, by letting the period tend to infinity; and second, by applying the improved long-wave limit approach to obtain lump waves. In the subsequent sections, we shall present some refined limiting procedures that overcome the aforementioned obstacles: the first step establishes the exact correspondence between lump chains and lump waves, while the second step identifies a perturbation strategy analogous to that in Eq. (15) that reduces lump chains directly to lump waves.

4. Reduction of two lump chains to three lump waves

Here, we first establish the correspondence between two lump chains and three lump waves, and then present a direct route to obtain lump waves from the two-lump-chain molecule. The two lump chains can be expressed via the Hirota transformation in Eq. (7)

$$f=\sum\exp\left(\sum_{i=1}^{4}v_iX_i+\sum_{i<j}^{4}v_iv_jA_{ij}\right), \tag{18}$$

where $X_1=X_3^*$, $X_2=X_4^*$, and all associated parameters for X_j and A_{ij} are specified in Eq. (10). With full generality retained, we set the parameters in Eq. (18) to the following values to simplify the analysis of this lump chain:

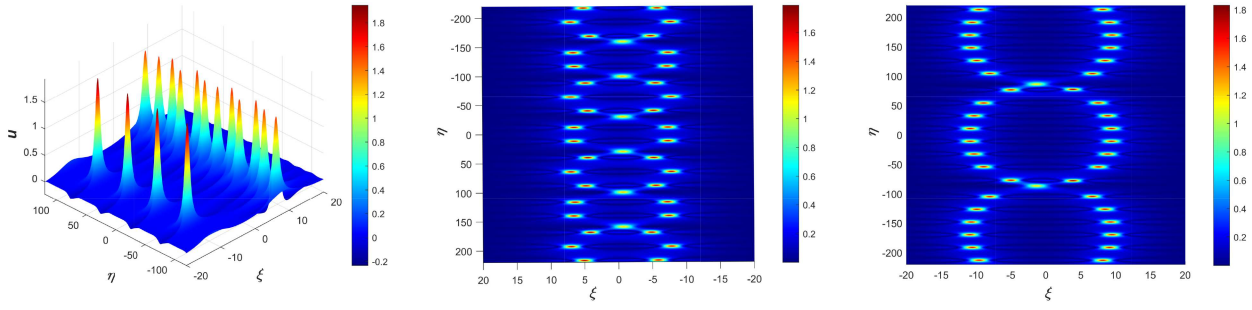
$$\theta_1=\theta_2=-1,\ \ \theta_3=\theta_4=1,\ \ k_1=k_3<k_2=k_4. \tag{19}$$

The period and amplitude of each lump chain are given by the following expressions:

$$T_j=\frac{2\pi}{k_j\sqrt{1-k_j^2}},\ \ A_j=\frac{3k_j^2}{1-\exp(-A_{j,j+2}/2)}, \tag{20}$$

and the periods of these lump chains are governed by the parameter k_j.

When $k_1\to k_2$, the amplitudes and periods of a pair of lump chains become increasingly close. Under this condition, the double lump chains shown in Fig. 3(a) gradually begin to couple, as shown in Fig. 3(b). When $\Delta k=k_2-k_1\to 0$, the spatial period of the coupling becomes increasingly larger, as shown in Fig. 3(b). Ultimately, in the limiting case where $k_1=k_2$, the lump chains are reduced to lump waves.



(a) (b) (c)

Fig. 3. As the parameters k_1 and k_2 approach each other, the degeneration process of the lump-chain molecule corresponding to Eq. (18) occurs. (a) $k_1=1/8$, $k_2=1/3$, $\Delta k=5/24$, $X_1=3/2$, and $X_2=-3/2$; (b) $k_1=101/400$, $k_2=11/30$, $\Delta k=137/1200$, $X_1=3/2$, and $X_2=7/5$; (c) $k_1=290/100$, $k_2=301/900$, $\Delta k=2/45$, $X_1=5/2$, and $X_2=5/2$.

To elaborate on the degeneration process of the two lump chains, we set the parameters of Eq. (18) as follows:

$$\begin{aligned}&\theta_1=\theta_2=1,\ \ \theta_3=\theta_4=-1,\\&k_2=k_1+\theta,\ \ k_3=k_1,\ \ k_4=k_3+\theta,\\&X_1^{(0)}=\omega_1^{(0)}+\ln\left(-\frac{\gamma}{\theta}\right),\ \ X_2^{(0)}=\omega_1^{(0)}+\ln\left(\frac{\gamma}{\theta}\right),\end{aligned}$$

$$X_3^{(0)}=\omega_1^{(0)}+\ln\left(-\frac{\gamma}{\theta}\right),\ \ X_4^{(0)}=\omega_1^{(0)}+\ln\left(\frac{\gamma}{\theta}\right), \tag{21}$$

where both γ and $\omega_1^{(0)}$ are arbitrary real parameters. Next, we consider the limiting case as $\theta\to 0$, while keeping the other parameters constrained by Eq. (19). Then the auxiliary function f in Eq. (18) degenerates into a new solution, which is

composed of two lump chains with identical spatial periods and amplitudes. This analytical solution can be expressed via the Hirota transformation in Eq. (7) as follows:

$$\begin{aligned} f \;=\; & -\gamma^2 B(k_3)\mathrm{e}^{2X_3} + \gamma\left(\frac{\mathrm{d}X_1}{\mathrm{d}k_1}\right)\mathrm{e}^{X_1} \\ & +2\frac{\partial}{\partial k_1}B(k_1,k_3)\mathrm{e}^{X_1+2X_3} + 1 \\ & -\gamma^3 B(k_1)B(k_1,k_3) \\ & \times\left[\left(\frac{\mathrm{d}X_3}{\mathrm{d}k_3}\right)B(k_1,k_3) + 2\frac{\partial}{\partial k_3}B(k_1,k_3)\right]\mathrm{e}^{X_1+2X_3} \\ & \times\gamma^4 B(k_1)B(k_1,k_3)^4\mathrm{e}^{2X_1+2X_2} \\ & -\gamma^3 B(k_1)B(k_1,k_3)\left(\left(\frac{\mathrm{d}X_1}{\mathrm{d}k_1}\right)B(k_1,k_3)\right. \\ & \left.+\left(\frac{\mathrm{d}X_1}{\mathrm{d}k_1}\right)\left(\frac{\partial}{\partial k_3}B(k_1,k_3)\right) + \frac{\partial^2}{\partial k_1\partial k_3}B(k_1,k_3)\right)\mathrm{e}^{X_1+X_3} \\ & +\gamma\left(\frac{\mathrm{d}X_3}{\mathrm{d}k_3}\right)\mathrm{e}^{X_3} + \gamma^2\left(\frac{\mathrm{d}X_3}{\mathrm{d}k_3}\right)\left(\frac{\mathrm{d}X_1}{\mathrm{d}k_1}\right)B(k_1,k_3) \\ & +\left(\frac{\mathrm{d}X_3}{\mathrm{d}k_3}\right)\left(\frac{\partial}{\partial k_1}B(k_1,k_3)\right) - \gamma^2 B(k_1)\mathrm{e}^{2X_1}\,|_{k_1=k_3}, \end{aligned} \tag{22}$$

where

$$B(k_1) = \frac{4k_1^2-3}{12k_1^2(k_1^2-1)},\;\; B(k_3) = \frac{4k_3^2-3}{12k_3^2(k_3^2-1)}.$$

$$B(k_1,k_3) = \frac{\sqrt{k_1^2-1}\sqrt{k_3^2-1}+2k_1^2-3k_1k_3+2k_3^2-1}{\sqrt{k_1^2-1}\sqrt{k_3^2-1}+2k_1^2+3k_1k_3-2k_3^2-1};$$

$$X_1 = \mathrm{i}k_1\eta\sqrt{1-k_1^2}+k_1\xi+\omega_1^{(0)},$$

$$X_3 = -\mathrm{i}k_3\eta\sqrt{1-k_3^2}+k_3\xi+\omega_3^{(0)}.$$

It should be emphasized that the perturbation technique for Eq. (21) was previously reported by Zhang *et al.*[28,29] In particular, with $k_1 = 1/10$, $\omega_1^{(0)} = 0$, $\gamma = 1$, Eq. (22) can be written explicitly as follows:

$$\begin{aligned} f \;=\; & \frac{(121701888\eta^2+125452800\xi^2+79200000\xi+419080000)\mathrm{e}^{\frac{\xi}{5}}}{121651200}+1 \\ & -\frac{98\sqrt{11}\left(\mathrm{e}^{\frac{\xi}{10}}+\frac{10175\,\mathrm{e}^{\frac{3\xi}{10}}}{384}\eta\sin\left(\frac{3\eta\sqrt{11}}{100}\right)\right)}{165} - \frac{14800\mathrm{e}^{\frac{\xi}{5}}\cos\left(\frac{3\eta\sqrt{11}}{50}\right)}{297} + \frac{103530625\mathrm{e}^{\frac{2\xi}{5}}}{147456} \\ & +\frac{\left[(-6446880000\xi-4070000000)\,\mathrm{e}^{\frac{3\xi}{10}}+243302400\xi\mathrm{e}^{\frac{\xi}{10}}\right]\cos\left(\frac{3\eta\sqrt{11}}{100}\right)}{121651200}. \end{aligned} \tag{23}$$

This is a degenerate solution. It is composed of three fundamental types of functions: polynomials, trigonometric functions, and exponential functions. From a mathematical perspective, the degenerate solution Eq. (22) is essentially different from the lump-chain molecule Eq. (18), which is composed only of trigonometric and exponential functions. Lump-chain molecules are typically composed of lumps with different spatial periods and amplitudes. In contrast, the degenerate solution Eq. (22) is built from two lump chains whose periods and amplitudes are almost identical. As illustrated in Fig. 4(a), the single parameter k_1 simultaneously governs the period of both chains. When k_1 is decreased, the spatial period of the degenerate solution grows without bound, until, as captured in Fig. 4(c), the central expanse is reduced to a triumvirate of crests. Consequently, as the spatial periods of the two lump chains tend to infinity, we obtain a molecule consisting of exactly three lump waves. Therefore, in the limiting case $k_1 \to 0$, we can obtain a three-lump-wave structure similar to that depicted in Fig. 4(c). Crucially, however, lump-wave molecules are described solely by polynomials,[30] whereas the degenerate solution Eq. (22) additionally contains both trigonometric and exponential functions.

In mathematics, if we set the parameters in Eq. (22) as follows:

$$k_1 = \theta,\;\; \omega_1^{(0)} = a\theta^2+b\theta^3,\;\; \gamma = c\theta, \tag{24}$$

when $\theta \to 0$, the period of the solution of Eq. (22) gradually tends to infinity, and Eq. (22) can be reduced to a polynomial of degree six

$$\begin{aligned} f \;=\; & 14\xi^6+14(3\eta^2+29)\xi^4+168\xi^3 b \\ & +42(\eta^4+26\eta^2-36)\xi^2+168b(-3\eta^2+1)\xi \\ & +14\eta^6+238\eta^4+6384\eta^2+504b^2+24920, \end{aligned} \tag{25}$$

where $a = 1/3$ and $c = 2$. By setting the low-order terms of the series expansion of the degenerate solution Eq. (22) equal to zero, the parameters a, b, and c in Eq. (24) can be determined. When $k_1 \to 0$, the terms $B(k_1)$ and $B(k_3)$ in Eq. (22) are formally singular; however, since they are multiplied by γ^j, the products $\gamma^j B(k_1)$ and $\gamma^j B(k_3)$ remain bounded.

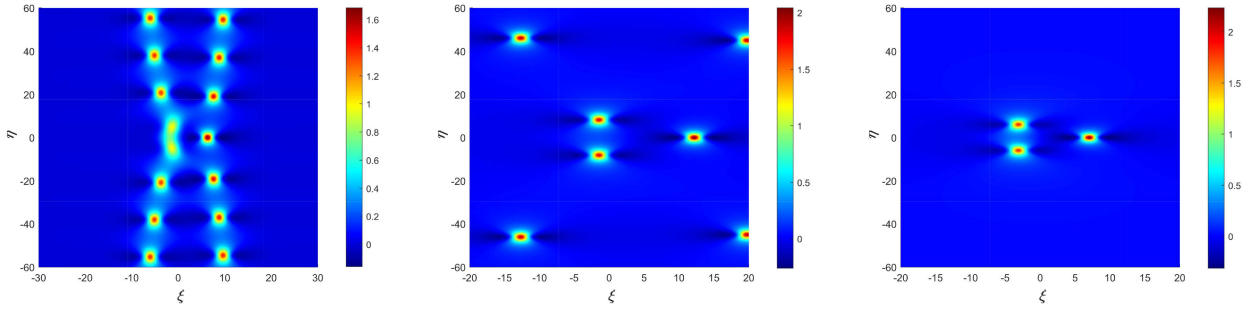
The derivation from Eq. (18) to Eq. (25) is rather lengthy and complex. We are concerned with whether there exists a simpler and more efficient method that allows us to derive lump-wave molecules directly from lump-chain molecules.

After surveying the literature,[23,30,31] we found a considerably simpler pathway. By setting the parameters as follows:

$$\theta_1 = \theta_2 = 1,\ \theta_3 = \theta_4 = -1,\ k_j = M_j\theta,$$
$$X_j^{(0)} = \omega_j^{(0)} + \alpha_j\theta^2 + \gamma_j\theta^3,\quad j = 1,2,3,4. \tag{26}$$

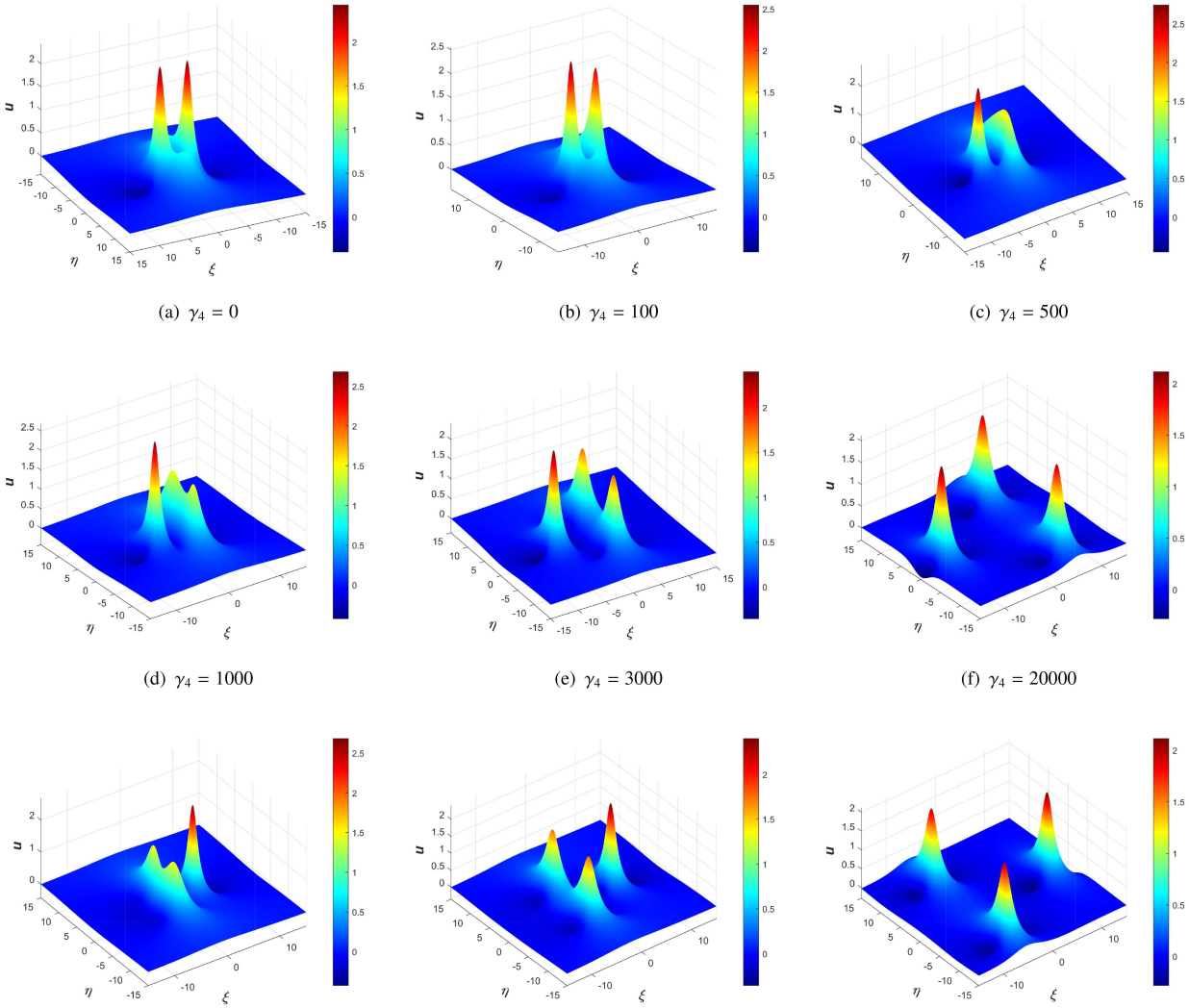
When $\theta \to 0$, we find that the exact analytical solution corresponding to Eq. (18) can be directly reduced to the lump waves. It can be written as the following sixth-degree polynomial via the Hirota transformation in Eq. (7)

$$\begin{aligned} f \ =\ & 150\xi^6 + 3750\xi^4 + 20\gamma_4\xi^3 - 18750\xi^2 - 20\gamma_4\xi \\ & +150\eta^6 + 2550\eta^4 + 71250\eta^2 + 450\xi^4\eta^2 + 450\xi^2\eta^4 \\ & +13500\xi^2\eta^2 - 60\gamma_4\xi\eta^2 + 281250 + 2/3\gamma_4^2, \end{aligned} \tag{27}$$



(a) (b) (c)

Fig. 4. (a) $k_1 = 2/5$; (b) $k_1 = 1/6$; (c) $k_1 = 1/11$.



(a) $\gamma_4 = 0$ (b) $\gamma_4 = 100$ (c) $\gamma_4 = 500$

(d) $\gamma_4 = 1000$ (e) $\gamma_4 = 3000$ (f) $\gamma_4 = 20000$

(g) $\gamma_4 = -1000$ (h) $\gamma_4 = -3000$ (i) $\gamma_4 = -20000$

Fig. 5. The figure shows that as the parameter γ_4 increases, the lump-wave molecule described by Eq. (27) evolves from the fundamental pattern shown in panel (a) to the triangular pattern shown in panel (f). A similar evolution occurs when the parameter γ_4 decreases from zero to large negative values, as illustrated in panels (g)–(i).

where

$$\gamma_1 = \frac{\gamma_4(M_1+M_2)M_1M_2}{(M_3+M_4)M_3M_4},\ \ \gamma_2 = \frac{\gamma_4(M_1+M_2)M_1M_2}{(M_3+M_4)M_3M_4},$$
$$\gamma_3 = \gamma_4,\ \ \omega_1^{(0)} = \ln\left(\frac{M_1+M_2}{M_1-M_2}\right),$$
$$\omega_2^{(0)} = \ln\left(-\frac{M_1+M_2}{M_1-M_2}\right),\ \ \omega_3^{(0)} = \ln\left(\frac{M_3+M_4}{M_3-M_4}\right),$$
$$\omega_4^{(0)} = \ln\left(-\frac{M_3+M_4}{M_3-M_4}\right),\ \ \alpha_1 = -\frac{M_1M_2(M_1-M_2)}{6(M_1+M_2)},$$
$$\alpha_2 = \frac{M_1M_2(M_1-M_2)}{6(M_1+M_2)},\ \ \alpha_3 = -\frac{M_3M_4(M_3-M_4)}{6(M_3+M_4)},$$
$$\alpha_4 = \frac{M_3M_4(M_3-M_4)}{6(M_3+M_4)}. \tag{28}$$

All parameters involved here are real numbers. The parameters M_j, $j = 1,2,3,4$, do not affect the solution Eq. (27). When the parameters M_j, $j = 1,2,3,4$ are mutually independent, the lump waves Eq. (27) can be derived from soliton solutions. When $M_1 = M_3$ and $M_2 = M_4$, Eq. (27) can be obtained from lump-chain solutions. The parameters $\omega_j^{(0)}$, α_j, γ_j, $j = 1,2,3,4$, in the expression are determined by requiring the low-order terms of the series expansion of Eq. (18) to vanish. As the parameter γ_4 increases gradually, the shape of the solution Eq. (27) evolves in a highly regular manner. When the parameter $\gamma_4 = 0$, a bimodal two-dimensional soliton can be obtained, with the two peaks being equal in amplitude, as shown in Fig. 5(a). As γ_4 gradually increases, the amplitude of the right-hand peak decreases, collapses, and splits into two smaller peaks, as illustrated in Figs. 5(b)–5(d). When γ_4 increases further, the amplitudes and shapes of the three wave peaks tend to become identical, as depicted in Fig. 5(f). As γ_4 decreases from zero toward negative infinity, a similar evolution occurs: the amplitude of the left front in the figure gradually diminishes and splits into two peaks, as shown in Figs. 5(g)–5(i). Analyzing the exact analytical solution of Eq. (27), we find that it remains invariant under the transformation $u(\xi,\eta,\gamma_4) = u(-\xi,-\eta,-\gamma_4)$, which partly explains the waveform's dependence on the parameter γ_4 depicted in Fig. 5. As shown in Fig. 5, when $|\gamma_4|$ tends to infinity, the distance between the lump waves gradually increases without bound.

5. Reduction of higher-order lump chains to multi-lump waves

The methods mentioned in the previous section can be extended to higher-order lump chains. In this section, we explain that the first path is theoretically feasible, but as the number of lump chains increases, the calculation becomes extremely complex. Therefore, we recommend the second path, which involves only a single limiting process to directly reduce Y-order lump chains to Y-order lump waves.

When $N = 2Y$, $X_j^* = X_{j+Y}^*$, $j = 1,2,\ldots,Y$, Eq. (10) can describe Y-order lump chains. In particular, when the relevant parameters are chosen as follows:

$$\theta_j = 1,\ \ \theta_{j+Y} = -1,\ \ k_i = k_{i+Y},\ \ X_j^{(0)} = X_{j+Y}^{(0)},$$
$$0 < k_j < 1/2,\ \ j = 1,2,\ldots,Y, \tag{29}$$

we can obtain three lump chains as illustrated in Fig. 6(a), which are parallel to one another and perpendicular to the ξ-axis.

The spatial period T_j and the amplitude A_j of each lump chain are both determined by the free parameter k_j, $j = 1,2,\ldots,Y$

$$T_j = \frac{2\pi}{k_j\sqrt{1-k_j^2}},\ \ A_j = \frac{3k_j^2}{1-\exp(-A_{j,j+M/2})},$$
$$j = 1,2,\ldots,Y. \tag{30}$$

As the parameters k_j approach each other, the periods and amplitudes of these lump chains also become close to each other, resulting in a coupling phenomenon and yielding coupled lump chains. Figure 6 illustrates the case $Y = 3$ in an intuitive way. As $|\,k_i - k_j\,|$ tends to zero, the coupled lump chains degenerate into lump waves.

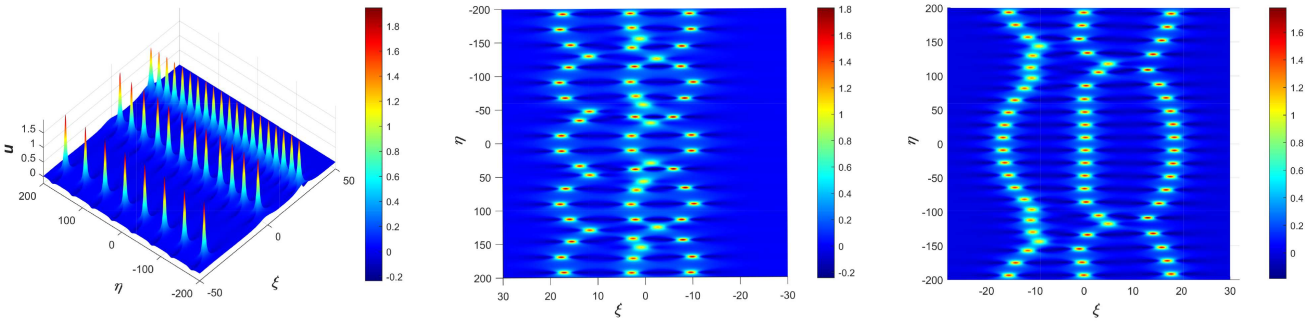


Fig. 6. (a) $N = 6$, $k_1 = 1/8$, $k_2 = 1/5$, $k_3 = 1/3$, $X_1^{(0)} = 5$, $X_2^{(0)} = 3$, and $X_3^{(0)} = -5$; (b) $N = 6$, $k_1 = 5/12$, $k_2 = 1/4$, $k_3 = 1/3$, $X_1^{(0)} = 3/2$, $X_2^{(0)} = 2$, and $X_3^{(0)} = 2$; (c) $N = 6$, $k_1 = 11/30$, $k_2 = 12/30$, $k_3 = 1/3$, $X_1^{(0)} = 5$, $X_2^{(0)} = 5$, and $X_3^{(0)} = 4$.

By using the improved long-wave limit method, we can readily obtain higher-order lump waves. The relevant parameters are set as follows:

$$\theta_1=\theta_2=\theta_3=1,\ \ \theta_4=\theta_5=\theta_6=-1,\ \ k_j=j\theta,$$
$$X_j^{(0)}=w_j^{(0)}+\alpha_j\theta^2+\beta_j\theta^3+\gamma_j\theta^4+\delta_j\theta^5,$$
$$j=1,2,\ldots,6, \tag{31}$$

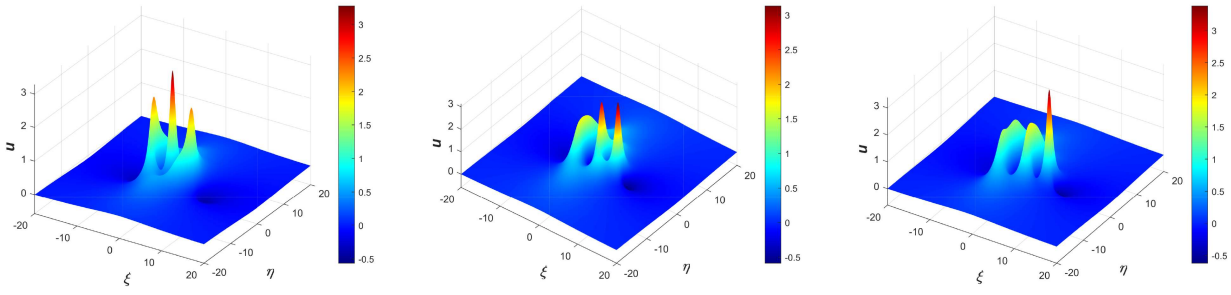
then, as $\theta\to 0$, the 6-soliton solution in Eq. (10) directly degenerates into a higher-order rational solution. The corresponding auxiliary function of this rational solution is a polynomial of degree 12.

$$\begin{aligned}
f=&+\frac{\left(475200\beta_2\delta_2+2673000\beta_2^2-1711998750\right)\xi^4}{3}+\frac{158400\eta^6\beta_2\xi^3}{3}\\
&+\frac{\left(950400\delta_2\beta_2^2-39600\beta_2^3-190159200\delta_2-8477931000\beta_2\right)\xi}{3}+19140\eta^{10}\\
&+\frac{\left(237600\delta_2+79200\beta_2\right)\eta^4\xi^3}{3}+\frac{\left(10929600\delta_2+170280000\beta_2\right)\eta^2\xi^3}{3}\\
&+\frac{\left(570240\delta_2^2-10454400\beta_2\delta_2-29205000\beta_2^2+99295927500\right)\eta^2}{3}+132000\beta_2^4\\
&+\frac{\left[-14553000\eta^4+\left(594000\beta_2^2+560290500\right)\eta^2+570240\delta_2^2+3801600\beta_2\delta_2\right]\xi^2}{3}\\
&+1430550\eta^8+\frac{\left(138600\beta_2^2+263663400\right)\eta^6}{3}+\frac{\left(-475200\beta_2\delta_2+4257000\beta_2^2\right)\eta^4}{3}\\
&+13780800\beta_2\delta_2+212993000\beta_2^2+\frac{5409269250\eta^4}{3}+570240\delta_2^2+\frac{96670862750}{3}\\
&+\frac{323400000\beta_2\xi^3}{3}+\frac{\left(5940\eta^{10}+564300\eta^8+35065800\eta^6-297000\beta_2^2\eta^4\right)\xi^2}{3}\\
&+\frac{\left(396000\beta_2^3+11642400\delta_2+323400000\beta_2\right)\xi^3}{3}+\frac{\left(39600\beta_2^3+11642400\delta_2\right)\xi^3}{3}\\
&+\frac{\left[(-2138400\delta_2+10494000\beta_2)\eta^4+(-1188000\beta_2^3-25423200\delta_2-794772000\beta_2)\eta^2\right]\xi}{3}\\
&+\frac{\left(66231000\beta_2^2+52729561500\right)\xi^2}{3}+\frac{\left[59400\eta^8\beta_2+\left(-237600\delta_2+4831200\beta_2\right)\eta^6\right]\xi}{3}\\
&+\frac{\left(-47520\delta_2-950400\beta_2\right)\xi^7}{3}+\frac{\left[19800\eta^6+1524600\eta^4+18433800\eta^2+59400\beta_2^2\right]\xi^6}{3}\\
&+8300600\xi^6+\frac{\left[118800\eta^4\beta_2+\left(427680\delta_2+2613600\beta_2\right)\eta^2-617760\delta_2-10335600\beta_2\right]\xi^5}{3}\\
&+\frac{\left[14850\eta^8+1445400\eta^6+37075500\eta^4+\left(89100\beta_2^2+218295000\right)\eta^2\right]\xi^4}{3}+\frac{96670862750}{3}\\
&+330\xi^{12}+\frac{\left(5940\eta^2+97020\right)\xi^{10}}{3}-6600\xi^9\beta^2+\frac{\left(14850\eta^4+683100\eta^2+727650\right)\xi^8}{3}+330\eta^{12},
\end{aligned} \tag{32}$$

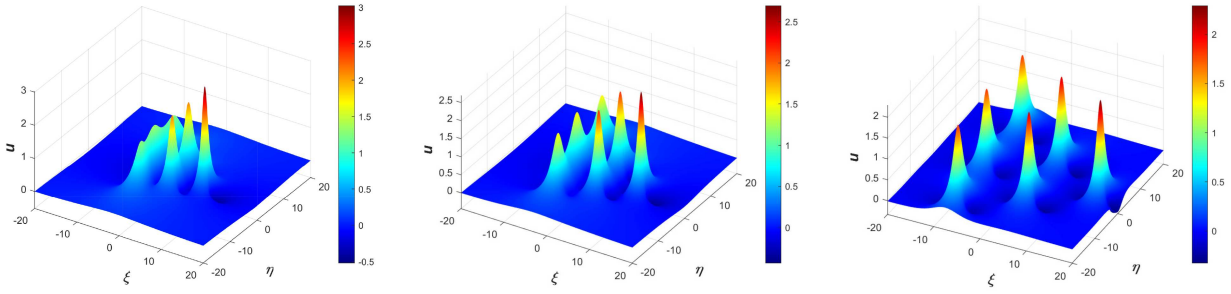
with

$$\begin{aligned}
&\exp^{(w_1^{(0)})}=-6,\ \ \exp^{(w_2^{(0)})}=15,\ \ \exp^{(w_3^{(0)})}=-10,\ \ \exp^{(w_4^{(0)})}=-45,\ \exp^{(w_5^{(0)})}=99,\ \ \exp^{(w_6^{(0)})}=-55,\\
&\alpha_1=1,\ \ \alpha_2=\frac{5}{3},\ \ \alpha_3=2,\ \ \alpha_4=2,\ \ \alpha_5=\frac{5}{3},\ \ \alpha_6=1,\ \ \delta_1=0,\ \ \delta_2=\delta_2,\ \ \delta_3=0,\ \ \delta_4=0,\ \ \delta_5=0,\ \ \delta_6=-44\delta_2,\\
&\gamma_1=3,\ \ \gamma_2=4,\ \ \gamma_3=-\frac{59}{18},\ \ \gamma_4=5,\ \ \gamma_5=6,\ \ \gamma_6=-\frac{667}{54},\ \ \beta_1=0,\ \ \beta_2=\beta_2,\ \ \beta_3=4\beta_2,\ \ \beta_4=0,\ \ \beta_5=\frac{15}{2}\beta_2,\ \ \beta_6=20\beta_2,
\end{aligned} \tag{33}$$

where β_2 and δ_2 are free real parameters that regulate the patterns of the lump-wave molecules. The parameters α_j, β_j, γ_j, δ_j, and $w_j^{(0)}$ in Eq. (33) are determined by setting the first few terms of the series expansion of Eq. (10) to zero. It merits emphasis that, although Pelinovskii *et al.*[30] first obtained higher-order lump-wave molecules from solitons or lump chains, these authors did not provide a detailed description of the solution process. The limiting trick employed in Eq. (31) is an extension of the work by Ablowitz *et al.*[23] Therefore, we refer to it as the improved long-wave limit method.

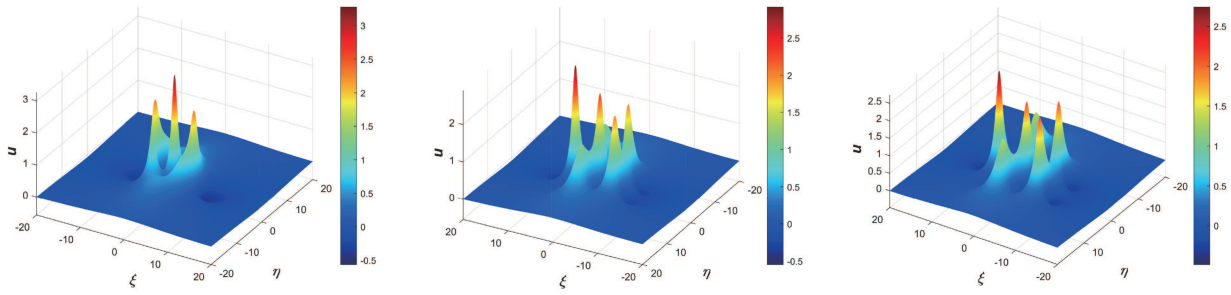


(a) $\beta_2 = 0$ (b) $\beta_2 = 10$ (c) $\beta_2 = 20$

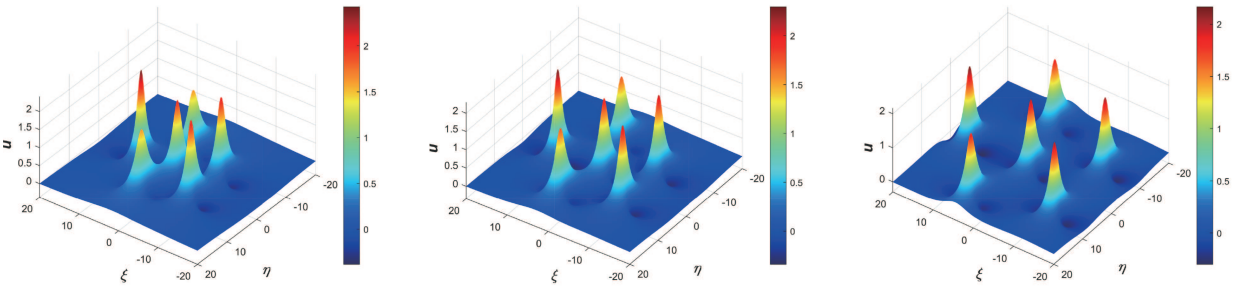


(d) $\beta_2 = 50$ (e) $\beta_2 = 100$ (f) $\beta_2 = 400$

Fig. 7. The figure illustrates that, for $\delta_2 = 0$, the lump-wave molecule governed by Eq. (33) undergoes a continuous deformation: with increasing β_2, it transitions from the elementary motif displayed in panel (a) to the sharply triangular configuration shown in panel (f).



(a) $\delta_2 = 0$ (b) $\delta_2 = 500$ (c) $\delta_2 = 1000$



(d) $\delta_2 = 4000$ (e) $\delta_2 = 10000$ (f) $\delta_2 = 40000$

Fig. 8. The figure reveals that, when $\beta_2 = 0$, the lump-wave molecule described by Eq. (33) undergoes a continuous geometric transition: with increasing δ_2, it deforms from the fundamental pattern depicted in panel (a) into the pentagonal mode illustrated in panel (f).

Since the third-order lump wave Eq. (32) contains an additional free parameter compared with the second-order lump wave Eq. (25), the variation of the free parameter can lead to more diverse molecular patterns. With $\delta_2 = 0$ and β_2 being gradually increased, the lump waves in Eq. (32) exhibit a tendency to form a triangular spatial configuration. At $\beta_2 = 0$, the solution reduces to the fundamental tri-peak soliton shown in Fig. 7(a). As β_2 grows, the left peak gradually collapses and splits into three peaks, while the middle peak gradually splits into two peaks, as shown in Figs. 7(b)–7(d). In the limit $\beta_2 \to \infty$, these six peaks tend to be of equal height, and we finally obtain the lump-wave molecule in a triangular pattern.

Figure 8 illustrates the influence of δ_2 on the solution with $\beta_2 = 0$. As δ_2 increases, the central peak of the three-peak

soliton gradually divides into three peaks, while the right peak gradually divides into two peaks. Thus, a pentagonal structure is formed in space, with each vertex and the center of the pentagon corresponding to a peak. In the limit $\delta_2 \to \infty$, these six peaks possess identical amplitudes and shapes.

By summarizing the results obtained in the preceding and present sections, we observe that if the parameters in Eq. (10) are assigned as follows:

$$\begin{aligned} &N = 2Y, \theta_j = 1, \quad \theta_{j+Y} = -1, k_j = k_{j+Y} = j\theta, \\ &j = 1, 2, \ldots, Y, \\ &X_j^{(0)} = X_{j+M}^{(0)^*} = \omega_j^{(0)} + A_{j,2}\theta^2 + A_{j,3}\theta^3 + \cdots \\ &\qquad + A_{j,2Y-2}\theta^{2Y-2} + A_{j,2Y-1}\theta^{2Y-1}. \end{aligned} \tag{34}$$

Consequently, as $\theta \to 0$, the Y-order lump chain collapses directly into the Y-order lump waves. To determine appropriate parameter values, we carry out a series expansion of solution Eq. (10) and set the first few terms of the series to zero. This yields a system of algebraic equations that can be readily solved to obtain the parameters ω_i and $A_{i,j}$. Then, Eq. (10) degenerates into a polynomial, and the degree of the polynomial is $Y(Y+1)$.

In principle, the method is capable of generating higher-order lump-wave molecules, yet as the order increases, the derivation becomes increasingly complicated. By juxtaposing the solutions exhibited in Figs. 5 and 7, we can draw the conclusion that parameter $A_{j,3}$ drives the higher-order rational solution from the multi-peak soliton shown in Figs. 5(a) and 7(a) into a triangular-patterned lump wave, while parameter $A_{j,5}$ transforms the multi-peak soliton in Fig. 8(a) into a pentagon-structured lump-wave molecule. In general, by controlling the parameters $A_{i,j}$, a wide variety of lump-wave molecular configurations can be obtained.

6. Conclusion

In this work, we propose two distinct methods for constructing multi-lump waves. The first method is to degenerate the lump chains into lump waves in two steps. In the first step, by choosing appropriate parameters to control the periods and amplitudes of the lump chains, the lump chains degenerate into an intermediate state composed of polynomials, exponential functions, and trigonometric functions when the periods and amplitudes of all lump chains tend to be identical. In the second step, when the periods of all lump chains in the intermediate state simultaneously tend to infinity, these lump chains finally degenerate into lump waves. In the second method, we directly degenerate the lump chains into lump waves using the improved long-wave limit approach, and we can obtain lump waves with various configurations by controlling the relevant free parameters. The improved long-wave limit method offers a markedly easier route to generating large-amplitude, rogue-wave-like multi-lump waves than the generalized Darboux-transformation framework.[32–36] It can furthermore be carried over to other integrable models — most notably the nonlinear Schrödinger equation[33] and its various extensions. Studies on lump chains[37] and lump waves[38–41] have recently gained widespread attention. The second method presented herein offers a notably simpler new route for continuing these investigations. The second method not only reveals the analytic bridge connecting solitons and lumps, but also reduces the computational overhead. Thereby, multi-lump waves can be generated more easily.

In future research, the analytical multi-lump-molecule solutions derived in this work can be compared with other types of localized coherent structures, such as super-regular breathers arising in PT -symmetric nonlinear systems.[42] In addition, physical-informed neural network techniques have been successfully applied to solving soliton equations and parameter identification,[43,44] and they can also be employed to numerically verify the dynamical stability of these lump-chain and multi-lump solutions in future studies.

Acknowledgments

Project supported by the National Natural Science Foundation of China (Grant Nos. 12575003, 12235007, and 12275144) and the K.C. Wong Magna Fund in Ningbo University.

References

[1] Fuchssteiner B and Tsegelnik V V 1995 *Theor. Math. Phys.* **105** 1354
[2] Ying Z L, Ming G C and Li H Y 2006 *Appl. Math. Lett.* **19** 808
[3] Liu X J, Zhou Y H, Zhang L, *et al.* 2014 *Sci. China Technol. Sci.* **57** 1285
[4] Zhang F, Hu Y R, Xin X P and Liu H Z 2022 *Comput. Appl. Math.* **41** 139
[5] Boussinesq J 1872 *J. Math. Pures Appl.* **17** 55
[6] Zakharov V E 1974 *Sov. Phys. JETP* **38** 108
[7] Bona J L and Sachs R L 1988 *Commun. Math. Phys.* **118** 15
[8] Deift P, Tomei C and Trubowitz E 1982 *Commun. Pure Appl. Math.* **35** 567
[9] Petviashvili V I 1976 *Fiz. Plazmy* **2** 469
[10] Satsuma J and Ablowitz M J 1980 *J. Fluid Mech.* **96** 731
[11] Matveev V B and Salle M A 1991 *Darboux Transformations and Solitons* (Berlin: Springer-Verlag)
[12] Zhang Z, Yang X Y, Li B, Guo Q and Stepanyants Y 2023 *Nonlinear Dyn.* **111** 1625
[13] Zhang Z, Li B, Chen J C, Guo Q and Stepanyants Y 2022 *Commun. Nonlinear Sci. Numer. Simul.* **112** 106555
[14] Zhang Z, Li B, Chen J C and Guo Q 2022 *Nonlinear Dyn.* **108** 4157
[15] Zhang Z, Guo Q and Stepanyants Y 2023 *Chaos, Solitons Fractals* **170** 113398
[16] Li W T, Lu C X and Li B 2024 *Nonlinear Dyn.* **112** 7359
[17] Li W T and Li B 2024 *Chaos, Solitons Fractals* **180** 114572
[18] Zhou Y, Manukure S and McAnally M 2021 *J. Geom. Phys.* **167** 104275
[19] Liu Y K, Li B and An H L 2018 *Nonlinear Dyn.* **92** 2061
[20] Hirota R 2004 *The Direct Method in Soliton Theory* (Cambridge: Cambridge University Press)

[21] Abramyan L A and Stepanyants Y A 1985 *Radiophys. Quantum Electron.* **28** 20

[22] Yuan F, Cheng Y and He J S 2020 *Commun. Nonlinear Sci. Numer. Simul.* **83** 105027

[23] Ablowitz M J and Satsuma J 1978 *J. Math. Phys.* **19** 2180

[24] Gdanov S K and Trubnikov B A 1984 *JETP Lett.* **39** 129

[25] Zaitsev A A 1983 *Sov. Phys. Dokl.* **28** 720

[26] Satsuma J and Ablowitz M J 1979 *J. Math. Phys.* **20** 1496

[27] Wang L H, He J S, Xu H, Wang J and Porsezian K 2017 *Phys. Rev. E* **95** 042217

[28] Zhang Z, Li B, Chen J C and Guo Q 2021 *Nonlinear Dyn.* **105** 2611

[29] Zhang Z, Chen J C and Guo Q 2022 *Commun. Theor. Phys.* **74** 045002

[30] Pelinovskii D E and Stepanyants Y A 1993 *JETP Lett.* **57** 24

[31] Liu M, Xu H and Wang Z 2023 *Int. J. Bifurcat. Chaos* **33** 2350164

[32] Wang L H, He J S, Xu H, Wang J and Porsezian K 2017 *Phys. Rev. E* **95** 042217

[33] Guo B L, Ling L M and Liu Q P 2012 *Phys. Rev. E* **85** 026607

[34] He J S, Zhang H R, Wang L H, Porsezian K and Fokas A S 2013 *Phys. Rev. E* **87** 052914

[35] Liu M Y, Xu H and Wang Z G 2023 *Int. J. Bifurcat. Chaos* **33** 2350164

[36] Xin X, Xia Y, Liu H and Zhang L 2020 *J. Math. Anal. Appl.* **490** 124227

[37] Lester C, Gelash A, Zakharov D and Zakharov V 2021 *Stud. Appl. Math.* **147** 1425

[38] Stepanyants Y A, Zakharov D V and Zakharov V E 2022 *Radiophys. Quantum Electron.* **64** 665

[39] Rao J G, He J S and Malomed B A 2022 *J. Math. Phys.* **63**

[40] Rao J G, Chow K W, Mihalache D and He J S 2021 *Stud. Appl. Math.* **147** 1007

[41] Zhang Z, Li B, Chen J C, Guo Q and Stepanyants Y 2022 *Phys. Scr.* **97** 115205

[42] Li X, Gao P and Liu W 2025 *Phys. Rev. A* **111** 033515

[43] Zhang Z, Liu M, Xing X, Zhang S, Yan Z and Liu W 2025 *Comput. Methods Appl. Mech. Eng.* **438** 117852

[44] Zhou H, Zhang Z, Liu M, Qi F and Liu W 2025 *Chin. Phys. Lett.* **42** 070001